NANO LETTERS

Letter

pubs.acs.org/NanoLett

Scalable Graphene Coatings for Enhanced Condensation Heat Transfer

Daniel J. Preston,[†] Daniela L. Mafra,[‡] Nenad Miljkovic,[†,§] Jing Kong,[‡] and Evelyn N. Wang*[,†]

[†]Department of Mechanical Engineering and [‡]Department of Electrical Engineering and Computer Science, Massachusetts Institute of Technology, Cambridge, Massachusetts 02139, United States

[§]Department of Mechanical Science and Engineering, University of Illinois, Urbana, Illinois 61801, United States

Supporting Information

ABSTRACT: Water vapor condensation is commonly observed in nature and routinely used as an effective means of transferring heat with dropwise condensation on nonwetting surfaces exhibiting heat transfer improvement compared to filmwise condensation on wetting surfaces. However, state-of-the-art techniques to promote dropwise condensation rely on functional hydrophobic coatings that either have challenges with chemical stability or are so thick that any potential heat transfer improvement is negated due to the added thermal resistance of the coating. In this work, we show the effectiveness of ultrathin scalable chemical vapor deposited (CVD) graphene coatings to promote dropwise condensation while offering robust chemical stability and maintaining low thermal resistance. Heat transfer enhancements of 4× were demonstrated compared to filmwise condensation, and the robustness of these CVD coatings was superior to typical hydrophobic monolayer coatings. Our results indicate that graphene is a promising surface coating to promote dropwise condensation of water in industrial conditions with the potential for scalable application via CVD.

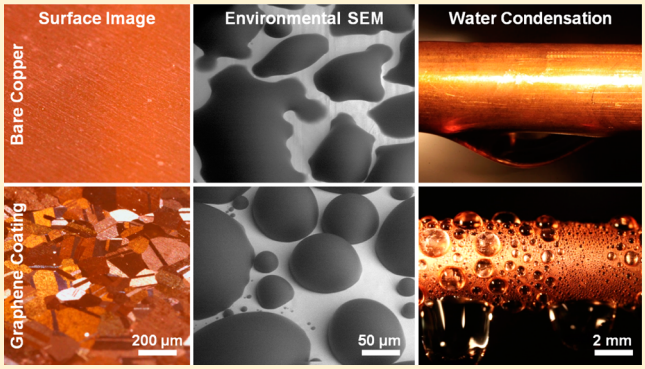

KEYWORDS: *Graphene, condensation, dropwise, heat transfer enhancement, robust, scalable*

Graphene is a two-dimensional material composed of carbon atoms arranged in a hexagonal lattice that has received significant attention since 2004 due to its unique and remarkable physical properties.[1] Prominent examples of the applicability of graphene include electronic device interconnects due to high charge carrier mobility,[2] transparent electrodes for solar cell devices,[3] and membranes for water desalination.[4] Graphene has also been used in thermal management applications due to its ability to improve device thermal conductivity and spread heat.[5] However, with graphene being a relatively new material, many applications have not yet been thoroughly explored.

One such application is the promotion of dropwise condensation. In typical industrial systems, condensed vapor forms a thin liquid film on the condenser surface due to the high surface energy associated with the majority of industrial heat exchanger materials (i.e., clean metals and metal oxides). This mode, known as filmwise condensation, is not desired due to the large thermal resistance to heat transfer.[6] Conversely, on low surface energy materials, the condensed vapor forms discrete liquid droplets. During this dropwise mode of condensation, droplets roll off at sizes approaching the capillary length (~2 mm for water) and clear the surface for renucleation, commonly resulting in 5−7× higher heat transfer performance compared to filmwise condensation.[7]

Dropwise condensation is typically achieved by functionalizing the condenser surface with a hydrophobic coating, for example, a fluorocarbon monolayer, wax, or polymer.[7a,8] Monolayer coatings (~1 nm thick) of long-chain fluorocarbons or fatty acids can induce hydrophobicity with negligible added thermal resistance but are often not robust, that is, chemically stable, over extended periods of time and therefore unsuitable in industrial applications.[7a,9] Thicker polymer coatings (>1 μm) such as PTFE have shown the potential to maintain robust hydrophobicity, but typically have a large thermal resistance that can negate the heat transfer enhancement gained by promoting dropwise condensation.[7a] More recently developed methods such as initiated chemical vapor deposition (iCVD) and plasma enhanced chemical vapor deposition (PECVD) have been used to grow ultrathin (<40 nm) conformal polymer coatings with success in achieving dropwise condensation.[9b,10] However, the durability of iCVD and PECVD coatings requires further characterization due to limited extended testing to assess mechanical wear and chemical stability for long-term condensing applications.

Received: December 2, 2014
Revised: March 22, 2015
Published: March 31, 2015

DOI: 10.1021/nl504628s
Nano Lett. 2015, 15, 2902−2909

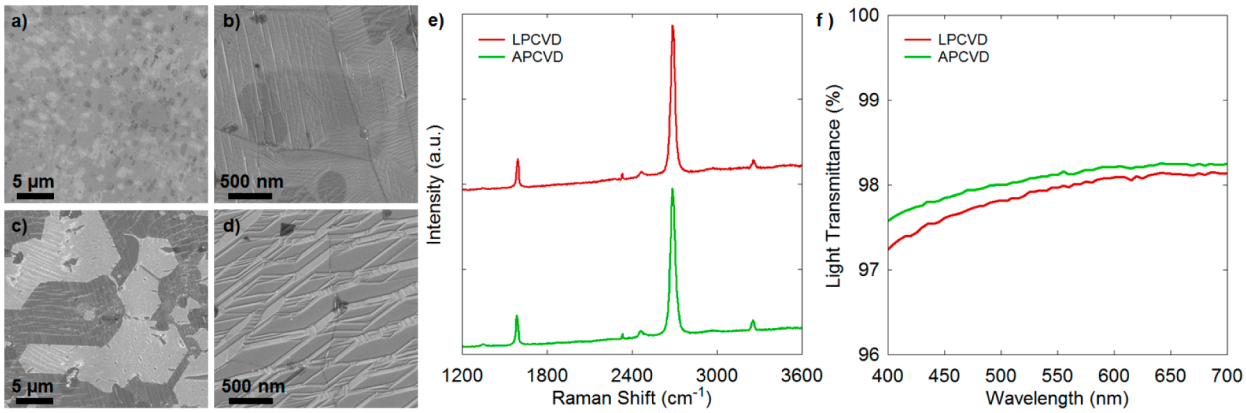

Figure 1. Field emission scanning electron microscopy images for (a,b) the low-pressure CVD graphene coating and (c,d) the atmospheric pressure CVD graphene coating on high-purity (>99.99%) copper substrates. During growth, the native copper oxide layer is reduced by H_2 gas at high temperature, and the underlying copper forms pronounced grains. Upon exposure to CH_4 at 1000 °C, graphene islands nucleate and grow over the surface until colliding with other islands. The copper grains remain visible. (e) Representative Raman spectra for the CVD graphene layers after transfer to a silicon substrate, obtained with a confocal Raman microscope using a 532 nm laser, demonstrate the presence of single-layer graphene for both CVD methods. (f) Optical characterization of the graphene transferred onto a transparent substrate indicated that both the LPCVD and APCVD graphene were predominately single-layer.[22]

Meanwhile, graphene displays hydrophobic behavior,[11] and its inert chemical nature and demonstrated mechanical strength suggest that it will resist degradation under typical condenser conditions.[3,12] Furthermore, the thermal resistance of a graphene coating is well-characterized[13] and is negligible in condensation applications (see Supporting Information, Section S2), and it can be applied relatively scalably via CVD.[14] Although graphene was initially suggested to have complete wetting transparency,[15] its hydrophobic nature has since been elucidated through careful experimental, numerical, and theoretical analysis.[11,16] Past work[15] also proposed graphene coatings to promote dropwise condensation, but the results of the experimental analysis did not show the expected improvement in heat transfer compared to filmwise condensation. The presence of noncondensable gases in the experimental setup not only reduced the improvement gained by promoting dropwise condensation to 30−40% as opposed to 500−700% but also resulted in reported condensation heat transfer coefficients 3 orders of magnitude lower than typical values without noncondensable gases.[7a] Furthermore, the mechanism for the dropwise condensation behavior was attributed to the "transparent" graphene layer protecting the copper from oxidation and preserving the intrinsic hydrophobic behavior of copper, while it has been demonstrated that copper is actually intrinsically hydrophilic[17] like other high-surface-energy materials.[18]

In this work, we demonstrated the uniform coating of high-purity (>99.99%) copper with graphene by both low and atmospheric pressure CVD. Both the low-pressure CVD (LPCVD) and the atmospheric pressure CVD (APCVD) graphene were single-layer. Subsequently, we experimentally demonstrated a 4× higher heat transfer coefficient for dropwise condensation of water on copper coated by graphene (both LPCVD and APCVD) compared to filmwise condensation on bare copper, which is in good agreement with theoretical models used for each case. The robustness of these graphene coatings was compared to a long-chain fluorocarbon monolayer commonly used to promote dropwise condensation, where 100 °C steam was condensed on both samples continuously. The fluorocarbon monolayer coating degraded completely in under 12 h, while for the graphene coatings, dropwise condensation was observed over a two-week span without showing signs of degradation. These results suggest that graphene is a robust and nonreactive coating material that enhances condensation heat transfer by promoting dropwise condensation.

The copper samples used as substrates for graphene CVD were high purity tubes (>99.99%, OD = 1/4 in., McMaster-Carr) and sections of sheet metal (>99.99%, thickness = 0.032 in., McMaster-Carr). Prior to the CVD process, the copper samples were sonicated in acetone, triple-rinsed with deionized water, submersed in 2.0 M hydrochloric acid, again triple-rinsed with deionized water, and finally treated for 10 min with argon plasma (Harrick PDC-001), which removes hydrocarbons via physical bombardment.[19] This process was also used to clean the bare copper samples for characterization of filmwise condensation under ideal conditions because past work has shown that bare copper exhibits filmwise condensation during continuous condensation.[20]

The CVD processes were then performed on the copper samples at both low and atmospheric pressure in a 1 in. quartz tube furnace. For both processes, the furnace was heated to 1000 °C, and hydrogen gas (with a flow rate of 10 sccm) for the LPCVD process and argon gas (with a flow rate of 500 sccm) for the APCVD process flowed over the samples for 30 min prior to graphene growth. Methane gas was then introduced and the synthesis of graphene was performed over 30 min at 1.9 Torr and atmospheric pressure for the LPCVD (with a flow rate of H_2/CH_4 = 70/4 sccm) and APCVD (with a flow rate of Ar/CH_4 = 500/3 sccm) coatings, respectively.[21] Finally, the samples were cooled to room temperature under hydrogen (10 sccm)/argon gas (500 sccm) for LPCVD/APCVD and then exposed to laboratory air (i.e., nonfiltered). While exposure to air leaves the possibility for contamination, the difference in wettability is expected to be negligible across different laboratory environments as indicated in past work[18b] (Further characterization specifically for graphene contamination under several different environments is an important topic and should be investigated in future research).

We characterized the samples using field-emission scanning electron microscopy (Zeiss Ultra-Plus) to determine the surface morphology, shown in Figure 1. Copper grains are visible on both the LPCVD and APCVD surfaces, and it was observed

DOI: 10.1021/nl504628s
Nano Lett. 2015, 15, 2902−2909

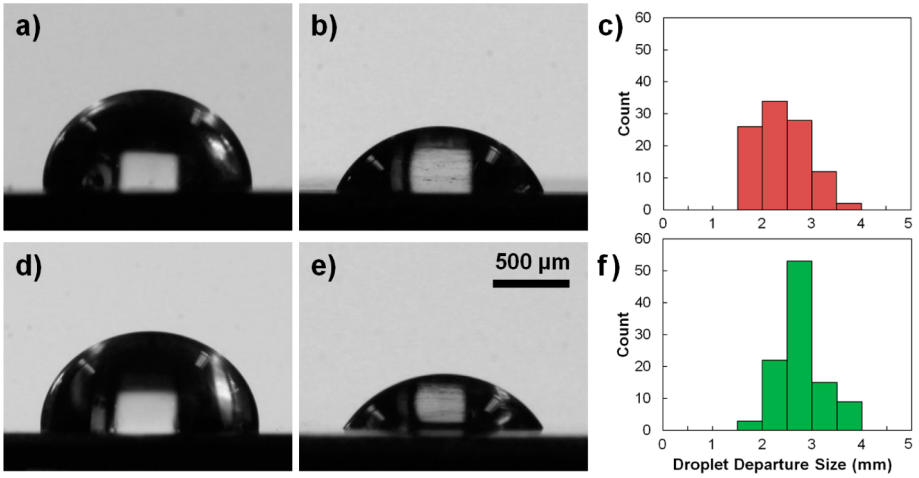

Figure 2. Representative images of (a) advancing and (b) receding contact angles of water on LPCVD graphene grown on a high-purity copper substrate, obtained by goniometric measurement. A histogram of droplet departure size during water condensation on LPCVD graphene is shown in (c). The advancing and receding contact angle for water on APCVD graphene are shown in (d) and (e), respectively, and a histogram of droplet departure size during water condensation on APCVD graphene is shown in (f). The average droplet departure diameter during water condensation on APCVD graphene is 2.8 ± 0.1 mm compared to 2.4 ± 0.1 mm on LPCVD graphene, suggesting a slightly higher expected condensation heat transfer coefficient on LPCVD graphene than on APCVD graphene.

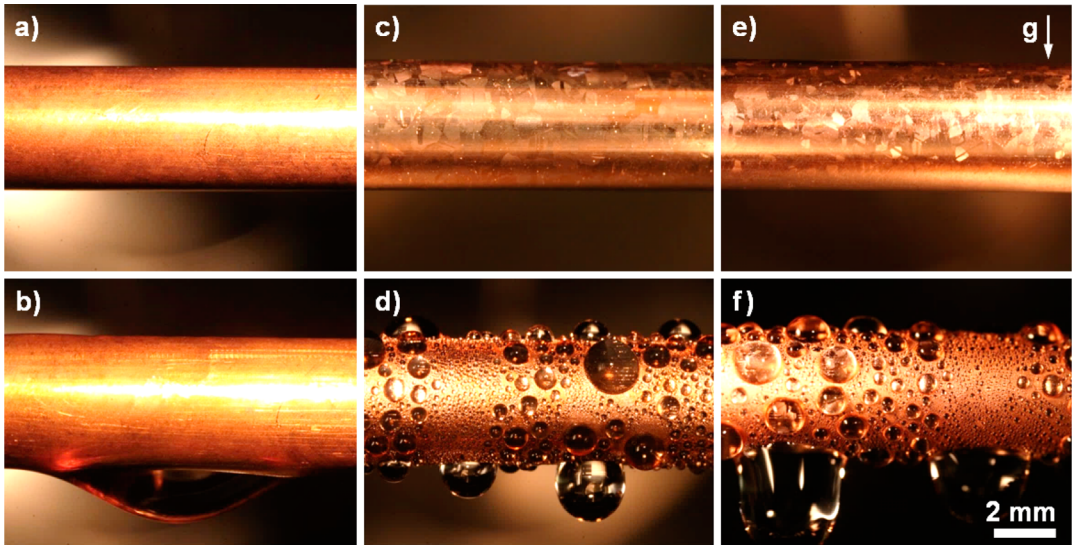

Figure 3. Photographs of a clean high-purity copper condenser tube (a) under vacuum and (b) undergoing filmwise condensation of deionized and degassed water vapor in the experimental vacuum chamber. Similarly, photographs of the graphene-coated high-purity copper condenser tubes are shown under vacuum and undergoing dropwise condensation of water with the LPCVD graphene coating in (c,d) and the APCVD graphene coating in (e,f).

that the graphene covered the entire surface of the copper. (The absence of visible copper grains on the bare copper surface is attributed to not heating the bare copper to 1000 °C as is required during graphene CVD.) Further characterization of the samples was conducted with Raman spectroscopy using a confocal Raman microscope with a 532 nm laser. Representative Raman spectra for the CVD graphene coatings after transfer onto a silicon substrate are shown in Figure 1e, where the ratio of 2D/G peaks (4−5×) and the full width at half-maximum of the 2D peak (25−30 cm^{-1}) demonstrate the presence of single-layer graphene for both CVD methods. Optical characterization of the CVD graphene after transfer onto a transparent substrate (see Supporting Information) was also performed to study the graphene thickness over a larger area than the Raman laser spot size (Raman spot size is ~1 μm while the transmittance measurement spot size is ~5 mm). The optical characterization indicated that both the LPCVD and APCVD graphene were predominately single-layer.[22]

We determined the surface wetting properties for water by goniometric characterization, where the advancing and receding contact angles in Figure 2 describe the surface wettability.[23] Both the advancing and receding contact angles need to be considered to determine the force that holds a droplet stationary on an inclined condensing surface against the force of gravity, which directly affects droplet departure size and condensation heat transfer.[24] The average advancing/receding contact angles were 87 ± 5°/64 ± 5° for the LPCVD graphene and 93 ± 5°/56 ± 5° for the APCVD graphene, determined from six points on each sample using a piezoelectric picoliter-scale droplet dispenser microgoniometer (Kyowa MCA-3) with

DOI: 10.1021/nl504628s
Nano Lett. 2015, 15, 2902−2909

the receding contact angle obtained during droplet evaporation and observed to exhibit constant receding contact angle behavior.[25] The contact angle hysteresis was attributed to sporadic defects on the surface, possibly at graphene grain boundaries. The droplet departure size during water vapor condensation, defined as the diameter at which droplets begin to slide down the condenser wall, is shown in Figure 2c,f. The average droplet departure diameters were 2.4 ± 0.1 mm on LPCVD graphene compared to 2.8 ± 0.1 mm on APCVD graphene, suggesting that the condensation heat transfer coefficient on LPCVD graphene will be slightly higher than on APCVD graphene as droplets shed at smaller sizes and refresh the surface for renucleation. The contact angle on the clean bare copper surface was ~0° with no distinction between advancing and receding.

We experimentally obtained the overall heat transfer performance of the graphene-coated copper tubes in a controlled vacuum chamber. Prior to condensation experiments, the vacuum chamber was evacuated to a pressure of $P <$ 1.0 Pa to eliminate the presence of noncondensable gases, which have been shown to severely degrade condensation heat transfer performance.[26] Water vapor was then introduced from a canister of degassed, deionized water attached to the vacuum chamber. The copper tube temperature was regulated by an internal chiller water flow loop which was isolated from the interior of the vacuum chamber, and the heat transfer through the tube wall was determined as a function of the chiller water flow rate and chiller water temperature at the tube inlet and outlet. As the copper tube was chilled internally, water vapor within the chamber condensed on the outer tube surface. The water vapor pressure within the chamber was maintained at values ranging from 2 to 5 kPa (corresponding to saturated water temperatures of 17 to 33 °C), which are typical for industrial condenser applications.[27]

Photographs of condensation on the exterior tube surfaces are shown in Figure 3. The bare copper tube underwent filmwise condensation of water vapor regardless of the temperature difference between the tube and the surrounding water vapor due to the spreading nature of water on clean copper (Figure 3a,b). The LPCVD (Figure 3c,d) and APCVD (Figure 3e,f) graphene coated tubes have visible graphene layers when dry (Figure 3c,e), and these coated tubes exhibited dropwise condensation over the full range of experimental conditions.

The overall heat flux, determined by the change in sensible heat of the chiller water, was obtained along with the log mean temperature difference (LMTD) between the chiller water and the temperature corresponding to the pressure of the surrounding water vapor for the bare copper (diamonds), LPCVD graphene (squares), and APCVD graphene (circles) (Figure 4a). The overall heat flux increased monotonically with the LMTD, where the local slope of this curve represents the overall heat transfer coefficient. Figure 4b shows the condensation heat transfer coefficient extracted from the overall heat transfer coefficient (see Supporting Information) as a function of vapor pressure while holding the supersaturation $S = P_{vapor}/P_{sat}(T_{wall})$ constant (S = 1.2). The theoretical predictions (dashed curves) were obtained from the droplet growth and distribution model for the graphene-coated condensers and from the Nusselt model for filmwise condensation on the bare copper condenser and were in good agreement with the experimental data (for model derivation and parameters, see Supporting Information). The assumption

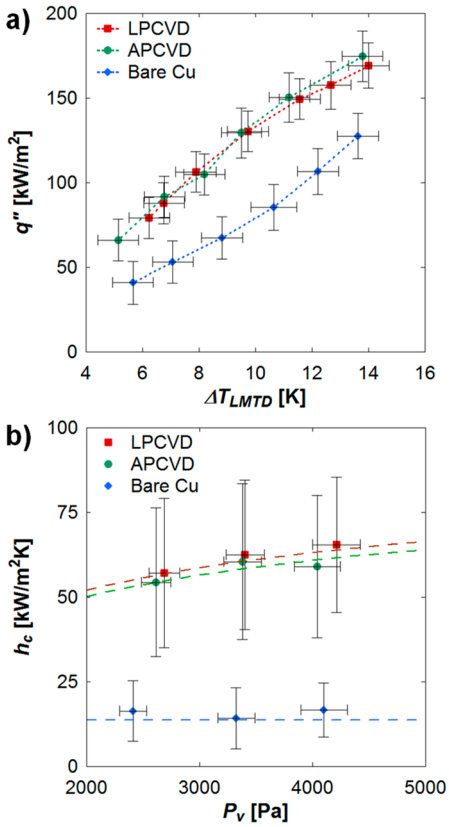

Figure 4. Water condensation heat transfer performance for the copper tubes with and without graphene coatings. The graphene-coated condensers exhibit dropwise condensation, while the bare copper undergoes filmwise condensation. Overall surface heat flux (q'') is shown as a function of the steady state experimental chiller-water-to-vapor log mean temperature difference (ΔT_{LMTD}) in (a), where the slope of the data trend represents the overall heat transfer coefficient, that is, the combination of the chiller water flow, copper tube, graphene coating (for coated tubes), and condensation heat transfer coefficients. (b) Experimental (points) and theoretical (dashed curves) steady-state condensation heat transfer coefficient (h_c), which includes graphene coatings where applicable, shown as a function of surrounding saturated vapor pressure (P_v). Error bars indicate the propagation of error associated with the fluid inlet and outlet temperature differential (±0.05 K) and pressure measurement (±2.5%). Theoretical predictions were obtained from the droplet growth and distribution model for the graphene-coated condensers with droplet departure size as an input parameter (for model derivation and parameters, see Supporting Information) and from the Nusselt model for filmwise condensation on the bare copper condenser.

of uniform wall temperature for the models was justified because the temperature variation in the chiller water from the inlet to outlet of the sample was over an order of magnitude less than the temperature difference from the sample to the surrounding vapor. The condensation heat transfer coefficient for the LPCVD and APCVD graphene coated copper tubes (~60 ± 20 kW/m^{2}K) was 4× greater than that measured for filmwise condensation on bare copper (~15 ± 9 kW/m^{2}K). Note that the dropwise condensation heat transfer coefficient decreases at low subcooling because the interfacial heat transfer coefficient becomes a major resistance to heat transfer,[7a,8e,28] while the filmwise condensation heat transfer coefficient increases at low subcooling as the film becomes thinner;[6] consequently, while a 4× enhancement was expected for the

DOI: 10.1021/nl504628s
Nano Lett. 2015, 15, 2902−2909

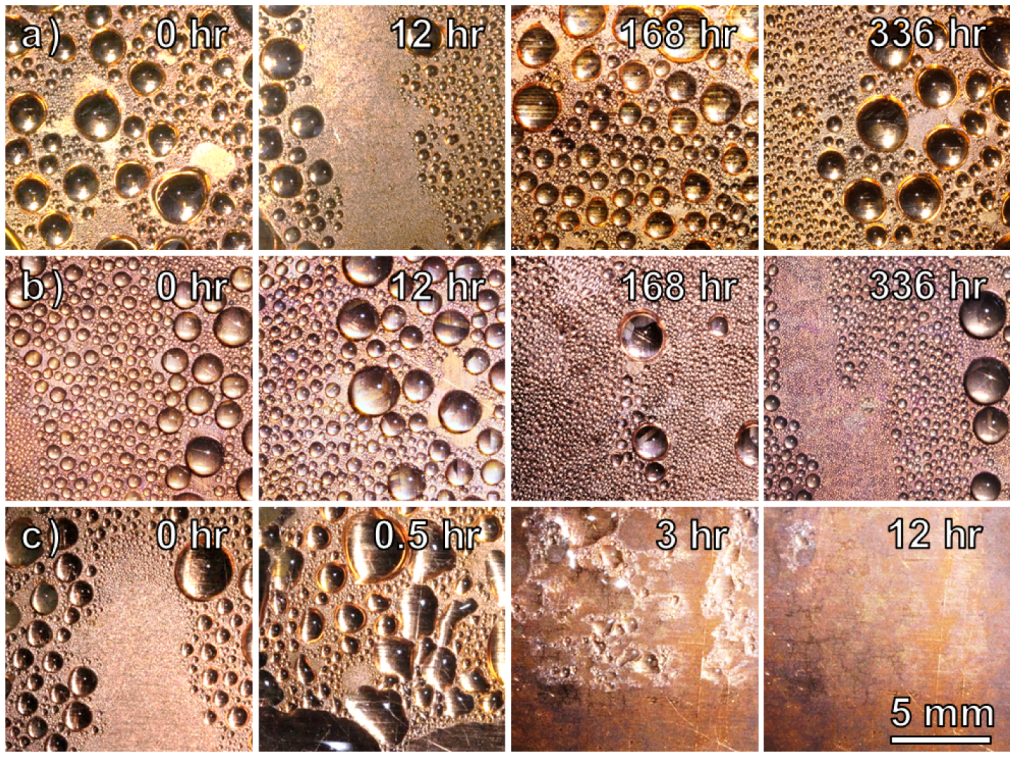

Figure 5. Time-lapse images of continuous condensation of 100 °C steam on (a) LPCVD, (b) APCVD, and (c) TFTS coatings on high-purity copper samples. The robust promotion of dropwise condensation by the graphene coatings is investigated over 2 weeks without showing signs of degradation, in contrast with the TFTS coating, which degraded and transitioned to filmwise condensation in less than 12 h.

subcooling range used to characterize the heat transfer coefficient in the present work (3.5−5 K), the typically reported 5−7× heat transfer coefficient enhancement[7a] would be realized at higher subcooling (over ∼10 K, see Supporting Information, Section S9).

The error for the condensation heat transfer coefficient was determined by propagating uncertainties associated with the chiller water thermocouples and mass flow meter, the pressure sensor inside the chamber, the sample surface area, and the Gnielinski correlation for heat transfer from the chiller water bulk to the internal surface of the sample. Since the condensation heat transfer coefficient, h_c, is not simply a function of a product of powers, the error must be determined from the first partial derivatives of h_c with respect to its components along with the uncertainties of its components (described in detail in the Supporting Information, Section S5).

In addition to improved condensation heat transfer by promoting dropwise condensation, graphene coatings also exhibit inert chemical behavior and excellent mechanical strength, which are expected to result in improved resistance to routine wear during condensation and provide a robust alternative to current state-of-the-art dropwise functionalization coatings. For direct comparison, a monolayer coating of trichloro(1H,1H,2H,2H-perfluorooctyl)silane (TFTS) was applied to a clean copper sample and, along with the graphene-coated samples, underwent an accelerated endurance test that consisted of continuous condensation of 100 °C steam. The TFTS coating was applied via vapor-phase deposition, where the copper substrate was cleaned as described for the graphene CVD, but oxygen plasma was substituted for argon plasma. The copper substrate was then placed in a desiccator immediately following the oxygen plasma treatment along with a vial containing 2 mL of TFTS. The desiccator was evacuated with a vacuum pump for 90 s, after which the sample was left in the TFTS vapor for 10 min. The sample was then removed from the desiccator, solvent rinsed, and dried with a clean nitrogen stream. The advancing/receding contact angles were 120 ± 5°/82 ± 5° on the TFTS-coated copper sample as fabricated.

The endurance test was performed in a controlled positive-pressure continuous condensation chamber (see Supporting Information, section S7). The samples were cooled to a surface temperature of 95 ± 1 °C and exposed to a continuous supply of 100 °C steam provided from a reservoir of degassed, deionized water. Initially, dropwise condensation was observed on both the LPCVD and APCVD graphene coated samples and the TFTS-coated sample (first column of Figure 5). However, the TFTS coating degraded noticeably within the first 30 min of testing with decreased advancing and receding contact angles observed, and completely transitioned to filmwise condensation within 12 h (Figure 5c), likely due to stripping of the coating by oxidation (X-ray photoelectron spectroscopy (K-Alpha) revealed that only 3% of the originally observed atomic percent of fluorine, a primary component of TFTS, remained on the surface after the continuous condensation experiment).[9c,29] Conversely, the LPCVD- and APCVD-graphene coated samples both sustained dropwise condensation for over 2 weeks with no signs of degradation when the experiments were discontinued (Figure 5a,b). Additionally, these graphene coatings can be altered to multilayer graphene or even single-/multilayer graphene composites[30] without drastic effect on the heat transfer (because the added thermal resistance is negligible, see Supporting Information Section S2) and can thus potentially be tailored to better prevent oxidation if it poses a problem. Further discussion on graphene's chemical robustness is presented in the Supporting Information, Section S8.

DOI: 10.1021/nl504628s
Nano Lett. 2015, 15, 2902−2909

While graphene offers a robust coating material to promote dropwise condensation on industrial metals, it is not a likely candidate to induce superhydrophobic behavior on micro- and nanostructured materials due to its relatively low advancing and receding contact angles compared to fluoropolymer coatings typically used for this application. While this eliminates the ability of graphene-coated surfaces to promote jumping droplet condensation,[31] the improvement in heat transfer coefficient of 4× provided by dropwise-promoting graphene coatings compared to filmwise condensation outweighs the marginal additional increase of 30−40% gained by jumping droplet condensation compared to dropwise condensation. Another potential limitation of these graphene coatings is their inability to induce dropwise condensation in systems that use low-surface-tension working fluids such as pentane; these fluids are expected to exhibit low contact angles and spread on graphene-coated surfaces, resulting in filmwise condensation.

This study demonstrates that graphene CVD coatings are a viable method to promote dropwise condensation of water in industrial conditions with a demonstrated improvement in heat transfer performance of 4× compared to clean industrial metals and superior robustness compared to state-of-the-art dropwise-promoting monolayer coatings as demonstrated under continuous condensation of 100 °C steam. This result promises significant energy savings in applications such as water harvesting, thermal management, industrial power generation, and building heating and cooling.

■ ASSOCIATED CONTENT

Supporting Information

ESEM characterization of the CVD graphene coatings, coating thermal resistance scaling, operation of the controlled condensation chamber for heat transfer measurement, calculation of condensation heat transfer coefficient and error analysis, modeling of condensation heat transfer coefficient, and operation of the robustness characterization setup. This material is available free of charge via the Internet at http://pubs.acs.org.

■ AUTHOR INFORMATION

Corresponding Author

*E-mail: enwang@mit.edu.

Author Contributions

E.N.W., J.K., D.J.P, and N.M. conceived the initial idea of this research. E.N.W. and J.K guided the work. D.L.M. and D.J.P. fabricated, functionalized, and characterized the experimental samples. D.J.P. carried out the experiments and collected and analyzed the data. D.J.P. and N.M. carried out the theoretical analysis. All authors were responsible for writing the paper and have given approval to the final version of the manuscript.

Notes

The authors declare no competing financial interest.

■ ACKNOWLEDGMENTS

We gratefully acknowledge funding support from the Office of Naval Research (ONR) with Dr. Mark Spector as program manager. We also acknowledge the support from the National Science Foundation through the Major Research Instrumentation Grant for Rapid Response Research (MRI-RAPID) for the microgoniometer. D.J.P. acknowledges funding received by the National Science Foundation Graduate Research Fellowship under Grant 1122374. Any opinion, findings, conclusions, or recommendations expressed in this material are those of the authors(s) and do not necessarily reflect the views of the National Science Foundation. D.L.M. acknowledges the Brazilian agency CNPq. J.K. acknowledges the support through the STC Center for Integrated Quantum Materials from NSF (U.S.) Grant DMR-1231319. This work was performed in part at the Center for Nanoscale Systems (CNS), a member of the National Nanotechnology Infrastructure Network (NNIN), which is supported by the National Science Foundation under NSF Award No. ECS-0335765. CNS is part of Harvard University.

■ ABBREVIATIONS

CVD, chemical vapor deposition; APCVD, atmospheric pressure CVD; LPCVD, low pressure CVD; FESEM, field emission scanning electron microscope; ESEM, environmental scanning electron microscope

■ REFERENCES

(1) (a) Novoselov, K. S.; Jiang, D.; Schedin, F.; Booth, T. J.; Khotkevich, V. V.; Morozov, S. V.; Geim, A. K. Two-dimensional atomic crystals. *Proc. Natl. Acad. Sci. U.S.A.* **2005**, *102* (30), 10451−10453. (b) Novoselov, K. S.; Geim, A. K.; Morozov, S. V.; Jiang, D.; Zhang, Y.; Dubonos, S. V.; Grigorieva, I. V.; Firsov, A. A. Electric field effect in atomically thin carbon films. *Science* **2004**, *306* (5696), 666−669.

(2) Chen, X. Y.; Akinwande, D.; Lee, K. J.; Close, G. F.; Yasuda, S.; Paul, B. C.; Fujita, S.; Kong, J.; Wong, H. S. P. Fully Integrated Graphene and Carbon Nanotube Interconnects for Gigahertz High-Speed CMOS Electronics. *IEEE Trans. Electron Dev.* **2010**, *57* (11), 3137−3143.

(3) (a) Li, X. S.; Zhu, Y. W.; Cai, W. W.; Borysiak, M.; Han, B. Y.; Chen, D.; Piner, R. D.; Colombo, L.; Ruoff, R. S. Transfer of Large-Area Graphene Films for High-Performance Transparent Conductive Electrodes. *Nano Lett.* **2009**, *9* (12), 4359−4363. (b) Wang, X.; Zhi, L. J.; Mullen, K. Transparent, Conductive Graphene Electrodes for Dye-Sensitized Solar Cells. *Nano Lett.* **2008**, *8* (1), 323−327.

(4) (a) Humplik, T.; Lee, J.; O'Hern, S. C.; Fellman, B. A.; Baig, M. A.; Hassan, S. F.; Atieh, M. A.; Rahman, F.; Laoui, T.; Karnik, R.; Wang, E. N. Nanostructured materials for water desalination. *Nanotechnology* **2011**, *22*, 292001. (b) O'Hern, S. C.; Stewart, C. A.; Boutilier, M. S. H.; Idrobo, J. C.; Bhaviripudi, S.; Das, S. K.; Kong, J.; Laoui, T.; Atieh, M.; Karnik, R. Selective Molecular Transport through Intrinsic Defects in a Single Layer of CVD Graphene. *ACS Nano* **2012**, *6* (11), 10130−10138.

(5) (a) Goli, P.; Ning, H.; Li, X. S.; Lu, C. Y.; Novoselov, K. S.; Balandin, A. A. Thermal Properties of Graphene-Copper-Graphene Heterogeneous Films. *Nano Lett.* **2014**, *14* (3), 1497−1503. (b) Malekpour, H.; Chang, K. H.; Chen, J. C.; Lu, C. Y.; Nika, D. L.; Novoselov, K. S.; Balandin, A. A. Thermal Conductivity of Graphene Laminate. *Nano Lett.* **2014**, *14* (9), 5155−5161. (c) Yan, Z.; Liu, G. X.; Khan, J. M.; Balandin, A. A. Graphene quilts for thermal management of high-power GaN transistors. *Nat. Commun.* **2012**, *3*, 827.

(6) Nusselt, W. The surface condensation of water vapour. *Z. Ver. Dtsch. Ing.* **1916**, *60*, 541−546.

(7) (a) Rose, J. W. Dropwise condensation theory and experiment: a review. *J. Power Energy* **2002**, *216* (A2), 115−128. (b) Schmidt, E.; Schurig, W.; Sellschopp, W. Condensation of water vapour in film- and drop form. *Z. Ver. Dtsch. Ing.* **1930**, *74*, 544−544.

(8) (a) Das, A. K.; Kilty, H. P.; Marto, P. J.; Andeen, G. B.; Kumar, A. The use of an organic self-assembled monolayer coating to promote dropwise condensation of steam on horizontal tubes. *J. Heat Transfer* **2000**, *122* (2), 278−286. (b) Marto, P. J.; Looney, D. J.; Rose, J. W.; Wanniarachchi, A. S. Evaluation of Organic Coatings for the Promotion of Dropwise Condensation of Steam. *Int. J. Heat Mass Transfer* **1986**, *29* (8), 1109−1117. (c) Vemuri, S.; Kim, K. J. An

DOI: 10.1021/nl504628s
Nano Lett. 2015, 15, 2902−2909

experimental and theoretical study on the concept of dropwise condensation. *Int. J. Heat Mass Transfer* **2006**, *49* (3−4), 649−657. (d) Vemuri, S.; Kim, K. J.; Wood, B. D.; Govindaraju, S.; Bell, T. W. Long term testing for dropwise condensation using self-assembled monolayer coatings of n-octadecyl mercaptan. *Appl. Therm Eng.* **2006**, *26* (4), 421−429. (e) Enright, R.; Miljkovic, N.; Alvarado, J. L.; Kim, K. J.; Rose, J. W. Dropwise Condensation on Micro- and Nanostructured Surfaces. *Nanoscale Microscale Thermophy. Eng.* **2014**, *18* (3), 223−250.

(9) (a) Boinovich, L. B.; Emelyanenko, A. M. Hydrophobic materials and coatings: Principles of design, properties and applications. *Usp. Khim.* **2008**, *77* (7), 619−638. (b) Paxson, A. T.; Yague, J. L.; Gleason, K. K.; Varanasi, K. K. Stable Dropwise Condensation for Enhancing Heat Transfer via the Initiated Chemical Vapor Deposition (iCVD) of Grafted Polymer Films. *Adv. Mater.* **2013**, *26* (3), 418−423. (c) Holden, K. M.; Wanniarachchi, A. S.; Marto, P. J.; Boone, D. H.; Rose, J. W. The Use of Organic Coatings to Promote Dropwise Condensation of Steam. *J. Heat Transfer* **1987**, *109* (3), 768−774.

(10) Miljkovic, N.; Preston, D. J.; Enright, R.; Wang, E. N. Electrostatic charging of jumping droplets. *Nat. Commun.* **2013**, *4*, 2517.

(11) (a) Raj, R.; Maroo, S. C.; Wang, E. N. Wettability of Graphene. *Nano Lett.* **2013**, *13* (4), 1509−1515. (b) Shin, Y. J.; Wang, Y. Y.; Huang, H.; Kalon, G.; Wee, A. T. S.; Shen, Z. X.; Bhatia, C. S.; Yang, H. Surface-Energy Engineering of Graphene. *Langmuir* **2010**, *26* (6), 3798−3802.

(12) (a) Li, X. L.; Zhang, G. Y.; Bai, X. D.; Sun, X. M.; Wang, X. R.; Wang, E.; Dai, H. J. Highly conducting graphene sheets and Langmuir-Blodgett films. *Nat. Nanotechnol.* **2008**, *3* (9), 538−542. (b) Blake, P.; Brimicombe, P. D.; Nair, R. R.; Booth, T. J.; Jiang, D.; Schedin, F.; Ponomarenko, L. A.; Morozov, S. V.; Gleeson, H. F.; Hill, E. W.; Geim, A. K.; Novoselov, K. S. Graphene-Based Liquid Crystal Device. *Nano Lett.* **2008**, *8* (6), 1704−1708.

(13) (a) Balandin, A. A. Thermal properties of graphene and nanostructured carbon materials. *Nat. Mater.* **2011**, *10* (8), 569−581. (b) Seol, J. H.; Jo, I.; Moore, A. L.; Lindsay, L.; Aitken, Z. H.; Pettes, M. T.; Li, X. S.; Yao, Z.; Huang, R.; Broido, D.; Mingo, N.; Ruoff, R. S.; Shi, L. Two-Dimensional Phonon Transport in Supported Graphene. *Science* **2010**, *328* (5975), 213−216. (c) Renteria, J. D.; Nika, D. L.; Balandin, A. A. Graphene Thermal Properties: Applications in Thermal Management and Energy Storage. *Appl. Sci.* **2014**, *4* (4), 525−547.

(14) (a) Hesjedal, T. Continuous roll-to-roll growth of graphene films by chemical vapor deposition. *Appl. Phys. Lett.* **2011**, *98*, 133106. (b) Bae, S.; Kim, H.; Lee, Y.; Xu, X. F.; Park, J. S.; Zheng, Y.; Balakrishnan, J.; Lei, T.; Kim, H. R.; Song, Y. I.; Kim, Y. J.; Kim, K. S.; Ozyilmaz, B.; Ahn, J. H.; Hong, B. H.; Iijima, S. Roll-to-roll production of 30-in. graphene films for transparent electrodes. *Nat. Nanotechnol* **2010**, *5* (8), 574−578.

(15) Rafiee, J.; Mi, X.; Gullapalli, H.; Thomas, A. V.; Yavari, F.; Shi, Y. F.; Ajayan, P. M.; Koratkar, N. A. Wetting transparency of graphene. *Nat. Mater.* **2012**, *11* (3), 217−222.

(16) (a) Shih, C. J.; Wang, Q. H.; Lin, S. C.; Park, K. C.; Jin, Z.; Strano, M. S.; Blankschtein, D. Breakdown in the Wetting Transparency of Graphene. *Phys. Rev. Lett.* **2012**, *109*, 176101. (b) Shih, C. J.; Strano, M. S.; Blankschtein, D. Wetting translucency of graphene. *Nat. Mater.* **2013**, *12* (10), 866−869.

(17) (a) Schrader, M. E. Ultrahigh-Vacuum Techniques in Measurement of Contact Angles 0.3. Water on Copper and Silver. *J. Phys. Chem.* **1974**, *78* (1), 87−89. (b) Trevoy, D. J.; Johnson, H. The Water Wettability of Metal Surfaces. *J. Phys. Chem.* **1958**, *62* (7), 833−837.

(18) (a) Bewig, K. W.; Zisman, W. A. Wetting of Gold and Platinum by Water. *J. Phys. Chem.* **1965**, *69* (12), 4238−4242. (b) Preston, D. J.; Miljkovic, N.; Sack, J.; Enright, R.; Queeney, J.; Wang, E. N. Effect of hydrocarbon adsorption on the wettability of rare earth oxide ceramics. *Appl. Phys. Lett.* **2014**, *105*, 11601. (c) Schrader, M. E. Wettability of Clean Metal-Surfaces. *J. Colloid Interface Sci.* **1984**, *100* (2), 372−380. (d) Schrader, M. E. Ultrahigh-Vacuum Techniques in Measurement of Contact Angles 0.2. Water on Gold. *J. Phys. Chem.* **1970**, *74* (11), 2313−2317. (e) Bernett, M. K.; Zisman, W. A. Confirmation of Spontaneous Spreading by Water on Pure Gold. *J. Phys. Chem.* **1970**, *74* (11), 2309−2312.

(19) (a) Umezu, I.; Kohno, K.; Aoki, K.; Kohama, Y.; Sugimura, A.; Inada, M. Effects of argon and hydrogen plasmas on the surface of silicon. *Vacuum* **2002**, *66* (3−4), 453−456. (b) Nickerson, R. Plasma surface modification for cleaning and adhesion. *Polymers, Laminations & Coatings Conference*, 1998; Tappi Press: Billerica, MA, Books 1 and 2; 1998; pp 1101−1108. (c) Wasy, A.; Balakrishnan, G.; Lee, S. H.; Kim, J. K.; Kim, D. G.; Kim, T. G.; Song, J. I. Argon plasma treatment on metal substrates and effects on diamond-like carbon (DLC) coating properties. *Cryst. Res. Technol.* **2014**, *49* (1), 55−62.

(20) (a) Erb, R. A. Wettability of Metals under Continuous Condensing Conditions. *J. Phys. Chem.* **1965**, *69* (4), 1306−1309. (b) Wilkins, D. G.; Bromley, L. A.; Read, S. M. Dropwise and Filmwise Condensation of Water Vapor on Gold. *AIChE J.* **1973**, *19* (1), 119−123. (c) Woodruff, D. W.; Westwater, J. W. Steam Condensation on Electroplated Gold - Effect of Plating Thickness. *Int. J. Heat Mass Tranfer* **1979**, *22* (4), 629−632.

(21) (a) Bhaviripudi, S.; Jia, X. T.; Dresselhaus, M. S.; Kong, J. Role of Kinetic Factors in Chemical Vapor Deposition Synthesis of Uniform Large Area Graphene Using Copper Catalyst. *Nano Lett.* **2010**, *10* (10), 4128−4133. (b) Li, X. S.; Cai, W. W.; An, J. H.; Kim, S.; Nah, J.; Yang, D. X.; Piner, R.; Velamakanni, A.; Jung, I.; Tutuc, E.; Banerjee, S. K.; Colombo, L.; Ruoff, R. S. Large-Area Synthesis of High-Quality and Uniform Graphene Films on Copper Foils. *Science* **2009**, *324* (5932), 1312−1314. (c) Reina, A.; Jia, X. T.; Ho, J.; Nezich, D.; Son, H. B.; Bulovic, V.; Dresselhaus, M. S.; Kong, J. Large Area, Few-Layer Graphene Films on Arbitrary Substrates by Chemical Vapor Deposition. *Nano Lett.* **2009**, *9* (1), 30−35.

(22) Nair, R. R.; Blake, P.; Grigorenko, A. N.; Novoselov, K. S.; Booth, T. J.; Stauber, T.; Peres, N. M. R.; Geim, A. K. Fine structure constant defines visual transparency of graphene. *Science* **2008**, *320* (5881), 1308−1308.

(23) (a) Gao, L. C.; McCarthy, T. J. Wetting 101 Degrees. *Langmuir* **2009**, *25* (24), 14105−14115. (b) Gao, L. C.; McCarthy, T. J. Contact Angle Hysteresis Explained. *Langmuir* **2006**, *22* (14), 6234−6237.

(24) (a) Miljkovic, N.; Enright, R.; Wang, E. N. Modeling and Optimization of Superhydrophobic Condensation. *J. Heat Transfer* **2013**, *135* (11), 111004−111004. (b) Kim, S.; Kim, K. J. Dropwise Condensation Modeling Suitable for Superhydrophobic Surfaces. *J. Heat Transfer* **2011**, *133* (8), 081502−1−081502−7. (c) Rose, J. W.; Glicksman, L. R. Dropwise condensation - the distribution of drop sizes. *Int. J. Heat Mass Tranfer* **1973**, *16*, 411−425. (d) Rumaa, J. Drop Size Distribution and Heat-Flux of Dropwise Condensation. *Chem. Eng. J.* **1978**, *16* (3), 171−176.

(25) Lam, C. N. C.; Wu, R.; Li, D.; Hair, M. L.; Neumann, A. W. Study of the advancing and receding contact angles: liquid sorption as a cause of contact angle hysteresis. *Adv. Colloid Interface Sci.* **2002**, *96* (1−3), 169−191.

(26) (a) Tanner, D. W.; Pope, D.; Potter, C. J.; West, D. Heat Transfer in Dropwise Condensation at Low Steam Pressures in Absence and Presence of Non-Condensable Gas. *Int. J. Heat Mass Tranfer* **1968**, *11* (2), 181−182. (b) Sundararaman, T. G.; Venkatram, T. Heat-Transfer during Dropwise Condensation of Steam in Presence of Non-Condensable Gases - Effects of Geometrical Shape of Surface Reversal of Cooling Water-Flow and Orientation. *Indian J. Technol.* **1976**, *14* (7), 313−321.

(27) (a) Vosough, A.; Falahat, A.; Vosough, S.; Esfehani, H. n.; Behjat, A.; Rad, R. n. Improvement Power Plant Efficiency with Condenser Pressure. *Int. J. Multidiscip. Sci. Eng.* **2011**, *2* (3), 38−43. (b) Bejan, A. Fundamentals of exergy analysis, entropy generation minimization, and the generation of flow architecture. *Int. J. Energy Res.* **2002**, *26* (7), 545−565.

(28) Wilmshurst, R.; Rose, J. W. *Dropwise Condensation—Further Heat Transfer Measurements*. In Fourth International Heat Transfer Conference; Elsevier: Paris-Versailles, 1970; Vol. 6.

DOI: 10.1021/nl504628s
Nano Lett. 2015, 15, 2902−2909

(29) Leidheiser, H. Corrosion of Painted Metals - a Review. *Corrosion* **1982**, *38* (7), 374−383.
(30) Shahil, K. M. F.; Balandin, A. A. Graphene-Multilayer Graphene Nanocomposites as Highly Efficient Thermal Interface Materials. *Nano Lett.* **2012**, *12* (2), 861−867.
(31) (a) Boreyko, J. B.; Chen, C. H. Vapor chambers with jumping-drop liquid return from superhydrophobic condensers. *Int. J. Heat Mass Tran* **2013**, *61*, 409−418. (b) Boreyko, J. B.; Chen, C. H. Self-Propelled Dropwise Condensate on Superhydrophobic Surfaces. *Phys. Rev. Lett.* **2009**, *103* (18), 184501−1−184501−4. (c) Miljkovic, N.; Enright, R.; Nam, Y.; Lopez, K.; Dou, N.; Sack, J.; Wang, E. N. Jumping-Droplet-Enhanced Condensation on Scalable Superhydrophobic Nanostructured Surfaces. *Nano Lett.* **2013**, *13* (1), 179−187. (d) Miljkovic, N.; Wang, E. N. Condensation heat transfer on superhydrophobic surfaces. *MRS Bull.* **2013**, *38* (5), 397−406.

DOI: 10.1021/nl504628s
Nano Lett. 2015, 15, 2902−2909